Measurement of the $dp \to {}^3\text{He}\eta$ reaction near threshold

J. Smyrski [a],[*], H.-H. Adam [b], A. Budzanowski [c], E. Czerwiński [a], R. Czyżykiewicz [a], D. Gil [a],
D. Grzonka [d], M. Janusz [a],[d], L. Jarczyk [a], B. Kamys [a], A. Khoukaz [b], P. Klaja [a],[d], T. Mersmann [b],
P. Moskal [a],[d], W. Oelert [d], C. Piskor-Ignatowicz [a], J. Przerwa [a],[d], B. Rejdych [a], J. Ritman [d], T. Rożek [e],
T. Sefzick [d], M. Siemaszko [e], A. Täschner [b], P. Winter [d], M. Wolke [d], P. Wüstner [f], W. Zipper [e]

[a] *Institute of Physics, Jagiellonian University, Pl-30-059 Cracow, Poland*
[b] *IKP, Westfälische Wilhelms-Universität, D-48149 Münster, Germany*
[c] *Institute of Nuclear Physics, Pl-31-342 Cracow, Poland*
[d] *IKP, Forschungszentrum Jülich, D-52425 Jülich, Germany*
[e] *Institute of Physics, University of Silesia, PL-40-007 Katowice, Poland*
[f] *ZEL, Forschungszentrum Jülich, D-52425 Jülich, Germany*

Received 22 February 2007; received in revised form 10 April 2007; accepted 13 April 2007

Available online 19 April 2007

Editor: V. Metag

Abstract

Total and differential cross sections for the $dp \to {}^3\text{He}\eta$ reaction have been measured near threshold for ${}^3\text{He}$ center-of-mass momenta in the range from 17.1 MeV/c to 87.5 MeV/c. The data were taken during a slow ramping of the COSY internal deuteron beam scattered on a proton target detecting the ${}^3\text{He}$ ejectiles with the COSY-11 facility. The forward–backward asymmetries of the differential cross sections deviate clearly from zero for center-of-mass momenta above 50 MeV/c indicating the presence of higher partial waves in the final state. Below 50 MeV/c center-of-mass momenta a fit of the final state enhancement factor to the data of the total cross sections results in the ${}^3\text{He}$–η scattering length of $|a| = 4.3 \pm 0.5$ fm.
© 2007 Elsevier B.V. All rights reserved.

PACS: 14.40.-n; 21.45.+v; 25.45.-z

Keywords: Meson production; Final state interaction; Eta-mesic nucleus

1. Introduction

Measurements of the $dp \to {}^3\text{He}\eta$ reaction near the kinematical threshold performed at the SPES-4 [1] and SPES-2 [2] spectrometers raised high interest due to a rapid increase of the total cross section very close to threshold. This increase, corroborated recently by the COSY-11 and ANKE groups [3,4], can be explained by the final state interaction (FSI) in the ${}^3\text{He}$–η system. The relatively large strength of this interaction led to the suggestion of a possible existence of a ${}^3\text{He}$–η bound state [5].

The measurements of the $dp \to {}^3\text{He}\eta$ reaction are insensitive to the sign of the scattering length and thus they do not allow to draw definite conclusions about possible bound states. However, they permit to determine the absolute value of the real part of the scattering length and the value of its imaginary part providing hints whether the necessary condition for the formation of a bound state ($|\text{Re}(a)| > \text{Im}(a)$) [6] is fulfilled.

The principal possibility for the creation of a η-mesic nucleus [7] attracts a lot of interest [8] still after twenty years of investigations. Present theoretical considerations reveal that the observation of such state would also deliver information about the flavour singlet component of the η meson [9]. Indications for the η-nucleus bound state were reported from the γ-${}^3\text{He}$ measurements [10], however, the data do not allow unambiguous conclusions [11].

[*] Corresponding author. Institute of Physics, Jagiellonian University, ul. Reymonta 4, Pl-30-059 Cracow, Poland. Tel.: +48 12 663 5616; fax: +48 12 634 2038.

E-mail address: smyrski@if.uj.edu.pl (J. Smyrski).

As a consequence of the attractive elementary η-nucleon interaction [12,13] the interaction of the η meson with the nucleus is expected to be attractive as well, yet the question whether its strength is sufficient to form a bound state remains still open. Recently Sibirtsev et al. [14] revised our knowledge of the ^{3}He–η scattering length via a systematic study of the available experimental data on the $dp \to {}^3\mathrm{He}\eta$ reaction [1,2,15,16]. The authors pointed out several discrepancies between various experiments. They suggest to perform measurements of angular distributions at excess energies around $Q = 6$ MeV, corresponding to a ^{3}He center-of-mass (c.m.) momentum of 74 MeV/c, in order to examine if there is a possible influence of higher partial waves already at this rather low energy. They also suggest measurements very close to threshold for putting more stringent constraints on the imaginary part of the scattering length. In order to resolve these inconsistencies and to check a possible onset of higher angular momenta, we performed high precision measurements of the total and differential cross sections for the $dp \to {}^3\mathrm{He}\eta$ reaction. Corresponding studies have also been conducted by the ANKE Collaboration [4].

2. Experiment

The experiment was performed with the internal deuteron beam of the Cooler Synchrotron COSY [17] scattered on a proton target of the cluster jet type [18] and the COSY-11 facility [19,20] detecting the charged reaction products. The nominal momentum of the deuteron beam was varied continuously within each acceleration cycle from 3.099 GeV/c to 3.179 GeV/c, crossing the threshold for the $dp \to {}^3\mathrm{He}\eta$ reaction at 3.140 GeV/c. Measurements below the threshold were used to search for a signal originating from decays of ^{3}He–η bound state in various channels like e.g. $dp \to {}^3\mathrm{He}\pi^0$ [21]. The data taken above threshold served for the present study of the $dp \to {}^3\mathrm{He}\eta$ reaction.

The ^{3}He ejectiles were momentum analysed in the COSY-11 dipole magnet and their trajectories were registered in two drift chambers. Identification of the ^{3}He ejectiles was based on the energy loss in scintillation counters and, independently, on the time-of-flight measured on a path of 9 m between two scintillation hodoscopes. The η mesons were identified via the missing mass technique. The luminosity was monitored using coincident measurement of the elastic d–p scattering and, independently, of the p–p quasi-free scattering. In both cases the forward scattered particles were measured in the drift chambers and the recoil particles were detected with silicon pad detectors.

Data taking during the ramping phase of the beam was already successfully conducted using the COSY-11 facility [22, 23]. Applications of this technique allow to eliminate most of the systematic errors which occur in case of setting up the beam for each momentum separately.

As the most serious source of systematic errors we consider the displacement of the beam position at the target correlated with variation of the beam momentum. Therefore, we monitored the beam position in the horizontal direction using measurements of p–p quasi-elastic scattering and d–p elastic scattering and applying methods described in Ref. [24]. In the
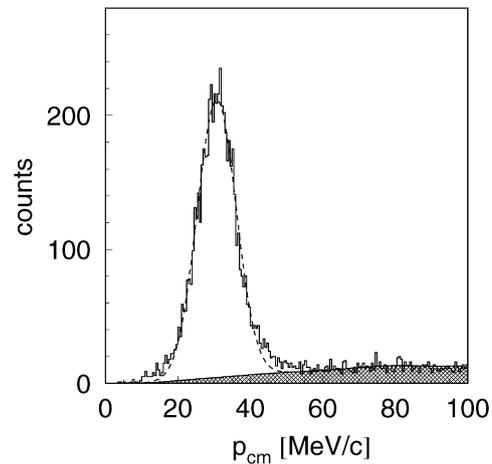

Fig. 1. Distribution of ^{3}He c.m. momenta for the nominal beam momentum interval: 3.147–3.148 GeV/c. The dashed line represents a Gaussian fit and the shaded area corresponds to the background measured below threshold.

vertical plane we used the reconstruction of the reaction vertices by tracing particle trajectories in the magnetic field of the COSY-11 dipole magnet. The precision of the beam position monitoring was ±0.5 mm horizontally and ±0.1 mm vertically.

3. Data analysis

During the off-line analysis the scanned beam momentum range from threshold up to 3.147 GeV/c was divided into 1 MeV/c intervals whereas above 3.147 GeV/c steps of 2 MeV/c were used. At the higher momenta the cross section depends only weekly on the beam momentum. For each interval the data analysis included the determination of: (i) the ^{3}He c.m. momentum – p_{cm}, (ii) the number of ^{3}He–η counts and (iii) the luminosity.

Due to the rapid variation of the near-threshold cross section for the $dp \to {}^3\mathrm{He}\eta$ process as a function of p_{cm}, a high precision knowledge of p_{cm} is extremely crucial for the present investigations. The nominal beam momentum in the range around 3.1 GeV/c calculated from the synchrotron frequency and the beam orbit length is known with an accuracy of 3 MeV/c only. The resulting uncertainty for $p_{\mathrm{cm}} = 32$ MeV/c is about $\Delta p_{\mathrm{cm}} = \pm12$ MeV/c. A much improved precision of p_{cm} can be reached on the basis of the extension of the ^{3}He kinematical ellipses measured via the momentum analysis in the magnetic field of the COSY-11 dipole magnet. We determined the absolute value of p_{cm} for the data collected for the nominal beam momentum interval of 3.147–3.148 GeV/c. The mean value of p_{cm} was calculated as the center of the Gaussian curve fitted to the peak corresponding to the ^{3}He–η production after subtraction of the multi-pion background measured below threshold (see Fig. 1). The systematic uncertainty of this procedure was tested using computer simulations of the experiment and was estimated as $\Delta p_{\mathrm{cm}} = \pm0.6$ MeV/c. The real beam momentum calculated from p_{cm} is by $\Delta p_{\mathrm{beam}} = 3.0 \pm 0.2 \pm 0.8$ MeV/c smaller than the nominal beam momentum, which is in line with results from previous experiments at COSY [16,25]. The indicated errors correspond to the uncertainty of p_{cm} and of
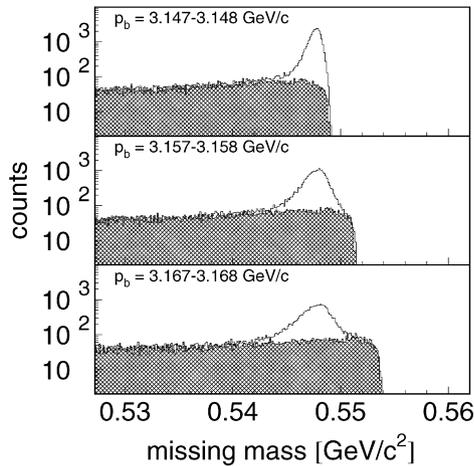
Fig. 2. Missing mass spectra for three different beam momentum intervals above the η production threshold. The shaded areas represent the multi-pion background measured below threshold which is scaled according to the luminosity and shifted to the kinematical limit of the missing mass.

the η mass (547.51 ± 0.18 MeV/c^2 [26]), respectively. The above difference was taken as a correction common for all nominal beam momenta, which is well justified since the relative changes of the COSY beam momentum during the ramping phase are controlled with a high accuracy of 1 keV/c per 1 MeV/c step.

In the missing mass spectra determined as a function of the beam momentum (see Fig. 2) a clear signal from the η meson production is seen. The background under the η peak is understood and can be very well reproduced and subtracted on the basis of measurements below threshold scaled according to the monitored luminosity and shifted to the kinematical limit of the missing mass. The correctness of this procedure was justified in Ref. [27]. For the determination of the angular distributions of the cross sections, the ^{3}He–η counts were determined individually for 10 bins of the full range of $\cos(\theta_{cm})$ where θ_{cm} is the ^{3}He emission angle in the c.m. system. The counts were then corrected for the COSY-11 differential acceptance which decreases from 100% at threshold to about 50% at the highest measured value of $p_{cm} = 87.56$ MeV/c.

An absolute value of the integrated luminosity was determined for a reference beam momentum interval of 3.147–3.148 GeV/c using the d–p elastic scattering. For this, the $dp \rightarrow dp$ differential counts registered in the range of four-momentum transfer $|t| = 0.6$–1.2 (GeV/c)^2 were compared with the d–p elastic cross section parametrised in Ref. [28] as: $d\sigma/dt = 487 - 353 \cdot |t|$ [μb/(GeV/c)^2]. The uncertainty of the integrated luminosity includes a statistical error of 3% and a systematic error of 9% due to the parametrisation. For the remaining beam momentum intervals, a relative integrated luminosity was determined with a high statistical accuracy of 0.3% by comparison of the p–p quasi-elastic counts with the ones for the reference interval.

4. Results and conclusions

Numbers of ^{3}He–η events corrected for the COSY-11 acceptance and normalised according to the integrated luminosity
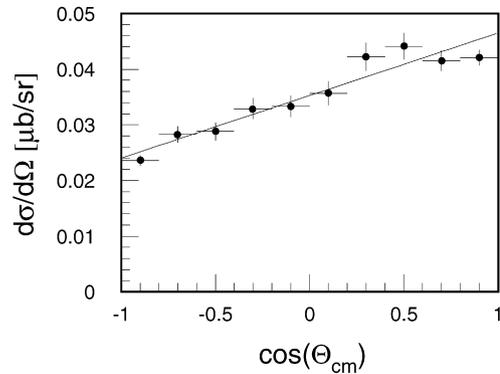

Fig. 3. Angular distribution of the cross section for nominal beam momentum from the interval 3.175–3177 GeV/c.

Table 1
Total cross sections and forward–backward asymmetries for the $dp \rightarrow {}^3$Heη reaction as a function of the c.m. momentum p_{cm}. The values of p_{cm} correspond to the central values the beam momentum intervals given in the first column. The listed errors represent statistical and systematic uncertainties, respectively. The overall normalisation error of the cross sections amounts to 12%

p_{beam} (GeV/c)	p_{cm} (MeV/c)	σ_{tot} (μb)	A
3.141–3.142	17.12	$0.323 \pm 0.004 \pm 0.004$	$-0.060 \pm 0.017 \pm 0.17$
3.142–3.143	22.66	$0.372 \pm 0.004 \pm 0.004$	$0.027 \pm 0.016 \pm 0.14$
3.143–3.144	27.07	$0.398 \pm 0.004 \pm 0.004$	$0.004 \pm 0.016 \pm 0.12$
3.144–3.146	32.61	$0.409 \pm 0.003 \pm 0.004$	$0.015 \pm 0.012 \pm 0.10$
3.146–3.148	38.77	$0.414 \pm 0.003 \pm 0.004$	$0.044 \pm 0.012 \pm 0.08$
3.148–3.150	44.09	$0.421 \pm 0.003 \pm 0.004$	$0.048 \pm 0.013 \pm 0.07$
3.150–3.152	48.82	$0.426 \pm 0.003 \pm 0.004$	$0.052 \pm 0.013 \pm 0.06$
3.152–3.154	53.14	$0.433 \pm 0.004 \pm 0.004$	$0.059 \pm 0.013 \pm 0.05$
3.154–3.156	57.13	$0.434 \pm 0.004 \pm 0.004$	$0.085 \pm 0.013 \pm 0.05$
3.156–3.158	60.86	$0.433 \pm 0.004 \pm 0.004$	$0.121 \pm 0.013 \pm 0.04$
3.158–3.160	64.38	$0.436 \pm 0.004 \pm 0.004$	$0.161 \pm 0.013 \pm 0.04$
3.160–3.162	67.71	$0.433 \pm 0.005 \pm 0.004$	$0.146 \pm 0.014 \pm 0.03$
3.162–3.164	70.88	$0.441 \pm 0.005 \pm 0.004$	$0.173 \pm 0.014 \pm 0.03$
3.164–3.166	73.92	$0.437 \pm 0.005 \pm 0.004$	$0.219 \pm 0.014 \pm 0.03$
3.166–3.168	76.85	$0.447 \pm 0.005 \pm 0.004$	$0.200 \pm 0.014 \pm 0.03$
3.168–3.170	79.66	$0.430 \pm 0.005 \pm 0.004$	$0.265 \pm 0.014 \pm 0.03$
3.170–3.172	82.37	$0.448 \pm 0.005 \pm 0.004$	$0.280 \pm 0.015 \pm 0.02$
3.172–3.174	85.01	$0.443 \pm 0.005 \pm 0.004$	$0.318 \pm 0.015 \pm 0.02$
3.174–3.176	87.56	$0.452 \pm 0.006 \pm 0.004$	$0.314 \pm 0.015 \pm 0.02$

were used for the determination of the angular distributions. These distributions can be well described by the linear function:

$$\frac{d\sigma}{d\Omega_{cm}} = \frac{\sigma_{tot}}{4\pi}\left[1 + A_{cm}\cos(\theta_{cm})\right], \quad (1)$$

where σ_{tot} is the total cross section and A_{cm} is the forward–backward asymmetry. An example of an angular distribution with the fitted linear function (1) is shown in Fig. 3. The values of σ_{tot} calculated by integrating the angular distributions and A_{cm} obtained from the linear fits with A_{cm} adjusted as a free parameter are given in Table 1 and are depicted in Figs. 4 and 5. The indicated uncertainties describe the statistical and systematic errors, respectively, the later resulting mainly from the uncertainty of the beam position at the target. The data points for the three lowest values of p_{cm} originate from an analysis of the data taken within the 1 MeV/c wide intervals of
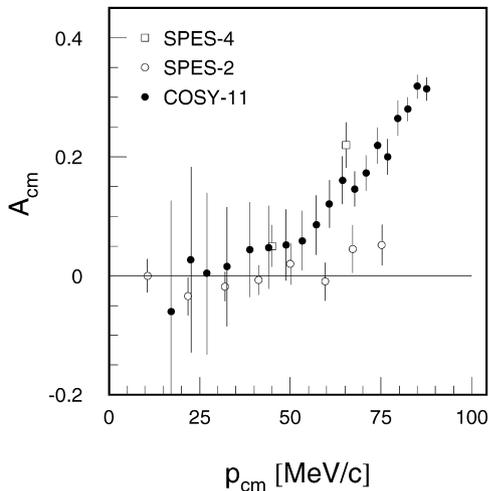
scattering length fit to the SPES-2 data [2] discussed below. The average cross section was calculated by integration over the beam momentum interval and over the total width of the beam momentum distribution:

$$\langle \sigma_{\text{tot}} \rangle = \frac{1}{\Delta} \int\limits_{p_0 - \Delta/2}^{p_0 + \Delta/2} dp' \frac{\int_{p'-\delta/2}^{p'+\delta/2} dp \, w(p - p') \sigma_{\text{tot}}(p)}{\int_{p'-\delta/2}^{p'+\delta/2} dp \, w(p - p')}, \qquad (2)$$

where Δ is the width of the beam momentum interval, δ is the total width of the beam momentum distribution and $w(p - p')$ is the distribution of the beam momentum p assumed to have a parabolic form: $w(p - p') = -1 \cdot (p - (p' - \frac{\Delta p}{2}))(p - (p' + \frac{\Delta p}{2}))$. Only for the lowest beam momentum interval the investigated difference $\sigma_{\text{tot}}(p_0) - \langle \sigma_{\text{tot}} \rangle$ is comparable with the experimental uncertainty of the cross section equal to 2.5% of σ_{tot}. For the intervals at higher beam momenta the differences are on the level of a few tens of % or even smaller and are negligible compared with the experimental uncertainties. Therefore, we neglect the effect of averaging over the beam momentum intervals and, further on, we consider obtained values of the total cross section as well as of the asymmetries as if they were taken at fixed beam momenta equal to the central values of the beam momentum intervals.

Our results on the forward–backward asymmetries are consistent with the points from SPES-4 measurements and, at lower momenta, also with the SPES-2 data, however, at higher momenta, they disagree with the SPES-2 results (see Fig. 4). They deviate clearly from zero for momenta above 50 MeV/c. This effect has been confirmed by the most recent results from the ANKE experiment [4] and it indicates a presence of higher partial waves in the final state which can result from the S- and P-wave interference.

As one can see in Fig. 5, our results for the total cross sections agree with the SPES-2 data. Comparing the present data to the SPES-4 points and to the results of previous COSY-11 measurements still a conformance within two standard deviations is observed.

In order to determine the ^{3}He–η scattering length we fitted the present data with an expression for the total cross section containing the enhancement factor describing the FSI, taken from Ref. [5]:

$$\sigma_{\text{tot}} = \frac{p_{\text{cm}}}{p_{\text{beam}}^{\text{cm}}} \left| \frac{f_B}{1 - i p_{\text{cm}} a} \right|^2, \qquad (3)$$

where f_B is the normalisation factor and a is the complex ^{3}He–η scattering length. A fit to the points for $p_{\text{cm}} < 50$ MeV/c, where the S-wave production dominates (see solid line in Fig. 5), results in: $|\text{Re}(a)| = 2.9 \pm 2.7$ fm and $\text{Im}(a) = 3.2 \pm 1.8$ fm at $\chi^2/n_{\text{free}} = 0.5$ in agreement with SPES-2 data from Ref. [2] of $|\text{Re}(a)| = 3.8 \pm 0.6$ fm and $\text{Im}(a) = 1.6 \pm 1.1$ fm. The obtained imaginary part of the scattering length is larger than the real one, however, due to the experimental uncertainties of these two values it is not possible to show that the necessary condition for the existence of a ^{3}He–η bound state ($|\text{Re}(a)| > \text{Im}(a)$) [6] is not fulfilled. The large uncertainties of $\text{Re}(a)$ and $\text{Im}(a)$ are connected with a very strong

Fig. 4. Forward–backward asymmetries in the c.m. system.

Fig. 5. Total cross section for the $dp \rightarrow {}^3$Heη reaction as a function of the ^{3}He c.m. momentum. The solid line represents the scattering length fit to the present data in the c.m. momentum range below 50 MeV/c and the dashed line results from the fit including data points at higher momenta. The star represents results of the previous COSY-11 measurement [3] which lie in the momentum range of the present experiment.

the beam momentum. The lowest interval was chosen in such a way that its distance from the threshold momentum exceeds one half of the total width of the beam momentum distribution. This guaranties, that the analysed data were taken exclusively above the threshold. The total width of the beam momentum distribution is 1.7 MeV/c and was determined on the basis of the monitored frequency spectrum of the COSY accelerator. It was confirmed by the observation of the η meson production at the central value of the beam momentum below the η production threshold.

Due to the strong non-linearity of the $dp \rightarrow {}^3$Heη cross section as a function of the beam momentum, the average values of the cross section, determined in the present analysis for the chosen finite beam momentum intervals, might differ from cross sections corresponding to the central beam momenta for the intervals. In order to estimate these differences we assumed that the momentum dependence of the cross section is given by the

correlation of these parameters, however, the absolute value of the scattering length could be determined much more precisely and is equal to $|a| = 4.3 \pm 0.5$ fm. The data points for $p_{cm} > 50$ MeV/c lie above the fitted line which can be caused by contributions from higher partial waves. Inclusion of these points in the fit results in a drastic increase of the χ^2/n_{free} value to 2.5.

Within the quoted uncertainties the data presented here agree with the one observed recently at ANKE [4]. However, at ANKE it was found that the extracted near-threshold cross sections can be described best by extending Eq. (3) by an effective range term, resulting in a much larger value for the scattering length. The data presented here can be described well without using additional parameters ($\chi^2/n_{free} = 0.5$). Further theoretical work on this exciting topic would be of great value.

Acknowledgements

References

[1] J. Berger, et al., Phys. Rev. Lett. 61 (1988) 919.
[2] B. Mayer, et al., Phys. Rev. C 53 (1996) 2068.
[3] H.H. Adam, et al., Phys. Rev. C 75 (2007) 014004.
[4] T. Mersmann, et al., nucl-ex/0701072.
[5] C. Wilkin, Phys. Rev. C 47 (1993) R938.
[6] Q. Haider, L.C. Liu, Phys. Rev. C 66 (2002) 045208.
[7] Q. Haider, L.C. Liu, Phys. Lett. B 172 (1986) 257.
[8] V. Baru, et al., nucl-th/0610011, Summary of the International Workshop on Eta-Nucleus Physics Held in Jülich, Germany, May 8–12, 2006.
[9] S.D. Bass, A. Thomas, Phys. Lett. B 634 (2006) 368.
[10] M. Pfeiffer, et al., Phys. Rev. Lett. 92 (2004) 252001.
[11] C. Hanhart, Phys. Rev. Lett. 94 (2005) 049101.
[12] P. Moskal, hep-ph/0408162.
[13] A.M. Green, S. Wycech, Phys. Rev. C 71 (2005) 014001.
[14] A. Sibirtsev, et al., Eur. Phys. J. A 22 (2004) 495.
[15] R. Bilger, et al., Phys. Rev. C 65 (2002) 44608.
[16] M. Betigeri, et al., Phys. Lett. B 472 (2000) 267.
[17] D. Prashun, et al., Nucl. Instrum. Methods Phys. Res., Sect. A 441 (2000) 167.
[18] H. Dombrowski, et al., Nucl. Instrum. Methods Phys. Res., Sect. A 386 (1997) 288.
[19] S. Brauksiepe, et al., Nucl. Instrum. Methods Phys. Res., Sect. A 376 (1996) 397.
[20] J. Smyrski, et al., Nucl. Instrum. Methods Phys. Res., Sect. A 541 (2005) 574.
[21] J. Smyrski, et al., Acta Phys. Slov. 56 (2006) 213.
[22] J. Smyrski, et al., Phys. Lett. B 474 (2000) 182.
[23] P. Moskal, et al., Phys. Rev. Lett. 80 (1998) 3202.
[24] P. Moskal, et al., Nucl. Instrum. Methods Phys. Res., Sect. A 466 (2001) 448.
[25] P. Moskal, et al., Phys. Rev. C 69 (2004) 025203.
[26] W.-M. Yao, et al., J. Phys. G 33 (2006) 1.
[27] P. Moskal, et al., J. Phys. G 32 (2006) 629.
[28] S. Steltenkamp, Diploma Thesis, Institut für Kernphysik, Westfälische Wilhelms-Universität Münster, 2002.